

A model-based approach for the rational design of the freeze-thawing of a protein-based formulation

Original

A model-based approach for the rational design of the freeze-thawing of a protein-based formulation / Arsiccio, A.; Marengo, L.; Pisano, R.. - In: PHARMACEUTICAL DEVELOPMENT AND TECHNOLOGY. - ISSN 1083-7450. - STAMPA. - 25:7(2020), pp. 823-831. [10.1080/10837450.2020.1743719]

Availability:

This version is available at: 11583/2862812 since: 2021-01-18T18:29:05Z

Publisher:

Taylor and Francis Ltd

Published

DOI:10.1080/10837450.2020.1743719

Terms of use:

This article is made available under terms and conditions as specified in the corresponding bibliographic description in the repository

Publisher copyright

GENERIC -- per es. Nature : semplice rinvio dal preprint/submitted, o postprint/AAM [ex default]

(Article begins on next page)

RESEARCH ARTICLE

A Model-Based Approach for the Rational Design of the Freeze-Thawing of a Protein-Based Formulation

Andrea Arsiccio, Livio Marengo and Roberto Pisano^a

^aDepartment of Applied Science and Technology, Politecnico di Torino, 24 corso Duca degli Abruzzi, Torino, 10129 Italy

ARTICLE HISTORY

Compiled April 28, 2020

ABSTRACT

Proteins are unstable molecules that may be severely injured by stresses encountered during freeze-thawing. Despite this, the selection of freeze-thaw conditions is currently empirical, and this results in reduced process control. Here we propose a mathematical model that takes into account the leading causes of protein instability during freeze-thawing, i.e., cold denaturation and surface-induced unfolding, and may guide the selection of optimal operating conditions. It is observed that a high cooling rate is beneficial for molecules that are extremely sensitive to cold denaturation, while the opposite is true when ice-induced unfolding is dominant. In all cases, a fast thawing rate is observed to be beneficial. The simulation outputs are confirmed by experimental data for myoglobin and lactate dehydrogenase, suggesting that the proposed modeling approach can reproduce the main features of protein behavior during freeze-thawing. This approach can therefore guide the selection of optimal conditions for protein-based formulations that are stored in a frozen or freeze-dried state.

KEYWORDS

freezing; thawing; proteins; Design Space; Quality by Design

1. Introduction

The rate of degradation processes is generally diminished in a frozen matrix, and this increases the shelf-life of frozen products. For this reason, protein-based drugs are often stored in the frozen state, or freeze-thawed during their processing and manipulation in industries and research institutions (Authelin et al. 2020). Freezing is also the first step of lyophilization, and preliminary freeze-thaw studies are often performed by lyo-experts to understand the effect of this process on protein-based formulations.

However, the conformational stability of a protein may be adversely affected by freeze-thawing because numerous mechanisms of denaturation may come into play. For instance, cold unfolding may occur at the low temperature experienced by the protein during a freeze-thaw cycle. This unfolding process is driven by the decreased penalty for the hydration of nonpolar groups at low temperatures; water molecules can, therefore, penetrate the hydrophobic core of the protein, promoting the sampling of non-native conformations (Davidovic et al. 2009; Matysiak et al. 2012; Privalov 1990; Lopez et al. 2008).

At the same time, the formation of ice crystals during freezing induces several modifications to the environment that surrounds the active ingredient. The ionic strength, pH, and composition may change because of cryoconcentration or phase-separation phenomena (Pikal-Cleland et al. 2000; Heller et al. 1996, 1997). The rate of chemical denaturation phenomena may even increase in a freeze-concentrated matrix (Pincock and Kiovsky 1966). The ice crystals themselves may act as a cause of unfolding. Direct adsorption onto the ice-water interface (Strambini and Gabellieri 1996), accumulation of air bubbles at the ice-freeze concentrate boundary (Schwegman et al. 2009; Authelin et al. 2020), high-pressure stresses during water crystallization, variations in pH, and excipient concentration (Bhatnagar et al. 2019) or enhanced cold denaturation at the ice surface (Arsiccio et al. 2020b) are possible theories to explain this observation.

It was observed that the formation of ice crystals was the primary source of protein denaturation for lactate dehydrogenase (Bhatnagar et al. 2008), and the azurin protein (Strambini and Gabellieri 1996), and this same behavior probably applies to many common pharmaceutical proteins. In line with these considerations, the formation of large ice crystals, and therefore small ice-water surface area was often found to significantly improve protein stability (Chang et al. 1996; Jiang and Nail 1998; Sarciaux et al. 1999). This result could be achieved by adjusting the cooling rate and the nucleation temperature (Jiang and Nail 1998; Eckhardt et al. 1991; Fang et al. 2018). A low cooling rate or a high nucleation temperature promotes the formation of large crystals (Searles et al. 2001; Bald 1986). It was for instance observed that the application of controlled nucleation techniques (Pisano 2019; Kasper and Friess 2011), which make it possible to trigger the formation of ice nuclei at high temperature, resulted in improved protein stability after freeze-thaw (Fang et al. 2018). The use of surfactants may also help in this case, as these molecules mitigate the risk of surface-induced denaturation (Lee et al. 2011; Chang et al. 1996; Arsiccio et al. 2018).

However, some other proteins were so prone to cold-denature that the critical processing parameter was not the extension of the ice-water surface area, but the time spent by the protein in a liquid matrix before cryoconcentration (Arsiccio et al. 2020a). In this case, a high cooling rate was observed to increase protein recovery after freeze-thawing.

The number of experimental observations supporting the idea that freeze-thawing may be detrimental for protein activity is therefore consistent. Despite the importance of the subject, a rational approach, based on an entirely mechanistic understanding of process phenomena, is not currently applied for the selection of optimal freeze-thaw conditions. In a previous work (Arsiccio et al. 2020a), we proposed a mathematical model that was oriented in this direction. The mechanisms of cold unfolding and surface-induced denaturation were coupled with a model of the freezing process, to identify different possible scenarios of protein instability. This model was framed in the broader context of Quality by Design (QbD) (Yu 2008; Yu et al. 2014), which highlights the importance of process control and robustness in pharmaceutical applications. In the QbD paradigm, mathematical modeling is recognized as an essential tool to increase the understanding of process behavior. In our previous work (Arsiccio et al. 2020a), we used the design space approach, which is a fundamental tool in the QbD framework, to explore the effect of different freezing conditions on protein recovery. However, the proposed model did not include any description of the thawing phase.

Here, we fill this gap by adding a mathematical description of protein behavior during thawing, as well, and we couple it with the previously developed model of the freezing step. This achievement would be relevant, especially considering that the thawing phase has often been observed to significantly influence protein stability (Cao

et al. 2003). For this purpose, we will again make use of the design space tool to make the selection of freeze-thaw conditions more robust. This work, therefore, adds value to and integrates the approach proposed in (Arsiccio et al. 2020a). In particular, the approach herein described may be extremely useful for protein-based formulations that are stored in a frozen or freeze-dried state, which include a high percentage of pharmaceutically relevant molecules.

The number and complexity of phenomena coming into play during freeze-thaw of a protein formulation are stunning and go beyond the possibility of an entirely mechanistic description. For this reason, approximations and assumptions will be made in the development of our approach. Nevertheless, the model outputs will be shown to allow a better understanding of experimental results obtained for myoglobin (Mb) and lactate dehydrogenase (LDH) as model proteins. This observation suggests that the direction taken by this first attempt to mathematically describe the freeze-thaw of proteins is correct, and the authors hope that this work will pave the way for further studies along these lines.

2. Materials and Methods

2.1. Mathematical Modeling

In this work, the thawing process of a protein formulation was modeled. A standard 4R vial, containing a 5% w/w sucrose formulation with a 150:1 sucrose to protein mole ratio was considered as a model system. We assumed to first freeze the solution by loading it onto a shelf whose temperature was decreased with a controlled ramp from 293 to 233 K, and then to thaw it by exposure to an external medium at 298 K. For the freezing step, different values of cooling rate and nucleation temperature in the range 0.1 - 1 K min⁻¹ or 248-265 K, respectively, were considered. This was done to simulate conditions resulting in different extensions of the ice-water surface area. The same model described in (Arsiccio et al. 2020a) was used for this purpose. Here, a thawing step was also added, and different values of heat transfer coefficient between the vial and the external medium were considered, in the range 5-100 W m⁻² K⁻¹. This was done to simulate thawing processes having different velocities. In all cases, a 2-state unfolding process was assumed, as it was done already in (Arsiccio et al. 2020a),



where N and U are the native and unfolded states, respectively.

For this simple, but yet realistic (Zwanzig 1997) 2-state system, the kinetics of unfolding can be readily described as,

$$\begin{aligned} \frac{d[U]}{dt} &= -k_f[U] + k_u[N] \\ \frac{d[N]}{dt} &= +k_f[U] - k_u[N] \end{aligned} \tag{2}$$

where k_f and k_u are kinetic constants that take into account all the parameters that influence protein stability, i.e., temperature T , concentration of stabilizers/denaturants

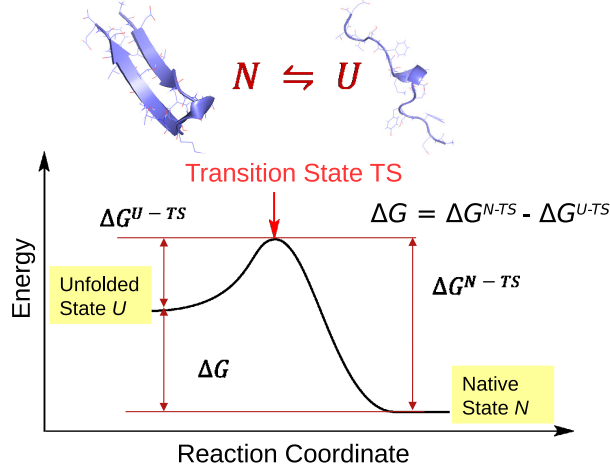


Figure 1. Scheme of the unfolding transition ($N \rightleftharpoons U$) of a protein, where the presence of an energy barrier, and the free energy differences between native, unfolded and transition states have been highlighted.

c and the solution viscosity μ . In particular, we could assume that the unfolding transition is an activated process, characterized by the presence of a transition state (see Figure 1). In this case, the kinetic constants would depend on the free energy difference between the native or unfolded state and the transition state ΔG^{X-TS} , with $X=U,N$ (see Figure 1).

$$\begin{aligned} k_u(T, c, \mu) &= D \frac{\mu_0}{\mu} e^{-\Delta G^{N-TS}/RT} \\ k_f(T, c, \mu) &= D \frac{\mu_0}{\mu} e^{-\Delta G^{U-TS}/RT} \end{aligned} \quad (3)$$

where D is a pre-exponential factor, μ_0 the viscosity at some reference conditions and R the universal gas constant. For this work, μ_0 was chosen as the viscosity of pure water at 293 K and 1 bar, so that $\mu_0 = 1$ cP.

The free energy change ΔG^{X-TS} is a function of the enthalpy ΔH_0^{X-TS} , entropy ΔS_0^{X-TS} and specific heat change Δc_p^{X-TS} of the transition,

$$\Delta G^{X-TS}(T, c) = \Delta H_0^{X-TS} - T\Delta S_0^{X-TS} + \Delta c_p^{X-TS}[T - T_0 - T \ln T/T_0] + m^{X-TS}c \quad (4)$$

where T_0 is a reference temperature, and m^{X-TS} is a proportionality coefficient which describes the effect of excipients on protein stability.

The values of ΔG^{X-TS} in a 2-step process are also related to thermodynamics by the relation $\Delta G = \Delta G^{N-TS} - \Delta G^{U-TS}$ (Figure 1), where ΔG is the free energy of unfolding,

$$\Delta G(T, c) = \Delta H_0 - T\Delta S_0 + \Delta c_p[T - T_0 - T \ln T/T_0] + mc \quad (5)$$

In this work, values of $0.2 \text{ kJ kmol}^{-1} \text{ K}^{-1}$, $3 \text{ kJ kmol}^{-1} \text{ K}^{-1}$ and 295 K were used for ΔS_0 , Δc_p and T_0 , as they result in realistic conditions of protein stability. By contrast, the values of ΔH_0 and m were varied among the different simulations here

Table 1. Protein stability parameters (ΔH_0 , m , D) used for the simulations performed in this work.

Sim. #	ΔH_0	m	D	Reversible
1	80	4	200	yes
2	60	1	200	yes
3	90	4	20	no
4	70	4	20	no

performed, to consider different situations of protein bulk stability, as detailed in Table 1. Both proteins that are stable (simulations 1 and 3) and unstable (simulations 2 and 4) in the bulk solution were considered. The kinetic constants k_u and k_f were finally computed assuming $\Delta G^{\text{N-TS}} = 1.5\Delta G$ and $\Delta G^{\text{U-TS}} = 0.5\Delta G$, while the constant D in Equation 3 was again changed between different simulations. Both the completely reversible situation, and the completely irreversible one were considered. In this last scenario Equations 3 reduce to,

$$\begin{aligned}\frac{d[\text{U}]}{dt} &= +k_u[\text{N}] \\ \frac{d[\text{N}]}{dt} &= -k_u[\text{N}]\end{aligned}\tag{6}$$

As evident from Equations 3 and 4, the evolution of temperature, excipient concentration and solution viscosity must be calculated to properly describe protein stability. All these parameters change during freezing and thawing. Modelling of the freezing phase was addressed in a previous work (Arsiccio et al. 2020a), and we will therefore focus here on the thawing phase.

The temperature evolution of the sample being thawed, from 233 K to ambient temperature, can be described taking into account two opposite contributions. The first is the heat provided by the external bath at temperature T_{ext} , and described by the heat transfer coefficient K_v . The second is the latent heat of fusion ΔH_f , which depends on the time evolution of the ice fraction X_{ice} (defined as the mass fraction of water that is in the solid state). It is therefore possible to write,

$$m_t c_p \frac{dT}{dt} = K_v A (T_{ext} - T) - \Delta H_f \frac{d(m_w X_{ice})}{dt}\tag{7}$$

where m_t is the total mass of the sample and m_w the mass of water, c_p the specific heat of the solution, T_{ext} the temperature of the external bath where the process is taking place. If we consider that the mass of water within the system m_w is a constant, and that the change of X_{ice} with time is due to the increase in product temperature, it is possible to write,

$$m_t c_p \frac{dT}{dt} = K_v A (T_{ext} - T) - \Delta H_f m_w \frac{dX_{ice}}{dT} \frac{dT}{dt}\tag{8}$$

The specific heat of the solution was calculated as an intermediate value between

those of ice, liquid water and sucrose,

$$m_t c_p = m_w X_{ice} c_{p,ice} + m_w (1 - X_{ice}) c_{p,w} + m_s c_{p,s} \quad (9)$$

where m_s is the mass of sucrose in the system. Values of $2108 \text{ J kg}^{-1} \text{ K}^{-1}$, $4186 \text{ J kg}^{-1} \text{ K}^{-1}$ and $1431 \text{ J kg}^{-1} \text{ K}^{-1}$ (Honig 2013) were used for $c_{p,ice}$, $c_{p,w}$ and $c_{p,s}$, respectively.

The mass fraction x_s of sucrose in the amorphous phase was calculated using the data from the sucrose-water phase diagram reported in Young and Jones (Young and Jones 1949). These data made it possible to compute the evolution of c during thawing, and also to estimate the variation in ice fraction X_{ice} with time. It is possible to write the following,

$$X_{ice} = 1 - \frac{m_s(1 - x_s)}{m_w x_s} \quad (10)$$

and therefore,

$$\frac{dX_{ice}}{dT} = \frac{m_s}{m_w x_s^2} \frac{dx_s}{dT} \quad (11)$$

Once the excipient concentration in the amorphous phase is known, it is also possible to compute its viscosity, for instance using the scaled Arrhenius equation,

$$\log_{10} \frac{\mu}{\mu_0} = c_0 + c_1 \left(\frac{T_g}{T} \right) + c_2 \left(\frac{T_g}{T} \right)^2 \quad (12)$$

where T_g is the glass transition temperature, and the coefficients c_0 , c_1 and c_2 were taken from (Longinotti and Corti 2008).

The initial extension of the ice water surface area was obtained from its value at the end of the freezing step (for details about the modelling procedure, see (Arsiccio et al. 2017)), while its decrease during heating of the solution was computed according to,

$$S_{ice}(t) = S_{ice}(t=0) \frac{x_{w,cryo}}{x_w(t)} \quad (13)$$

where $x_{w,cryo}$ is the liquid water mass fraction in the amorphous phase at the end of freezing, while x_w represents its current value. The percentage of protein molecules that denatured at the ice-water surface was calculated as described in (Arsiccio et al. 2020a). For this purpose, we assumed that surface-driven unfolding occurs with no barrier (i.e., $\Delta G = 0$, see Figure 1), and that 50% of the adsorbed molecules are therefore in the unfolded state.

All the equations listed above were solved in MATLAB R2017a, using a 0.1 s timestep. A scheme of the modelling approach used is shown in Figure 2.

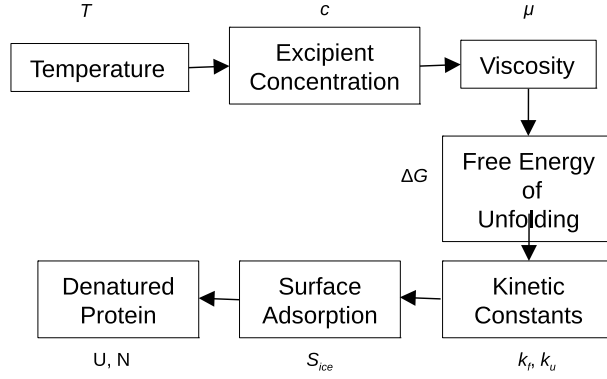


Figure 2. Scheme of the modelling approach used for the calculation of protein denaturation as a result of freeze-thawing.

2.2. Experimental Setup

2.2.1. Preparation of the Formulations

Myoglobin (Mb) from equine heart and L-lactic dehydrogenase from rabbit muscle (LDH, EC 1.1.1.27) were obtained from Sigma Aldrich (Milan, Italy) and used as model systems for this investigation. Myoglobin was solved in 10 mM sodium citrate buffer at pH 3.7 to obtain a final concentration of 0.1 mg/ml. Citrate buffer was selected because it does not undergo selective precipitation during freeze-thawing, thus allowing precise control of pH (Chang and Randall 1992). At the chosen value of pH, myoglobin is highly unstable, and cold denatures at high temperatures (283 K (Privalov 1997)). It was also shown in previous work that this unfolding process is extremely fast (Arsiccio et al. 2020a). This model system corresponds to the protein considered in simulations 2 and 4 in Table 1, i.e., to a molecule that is extremely sensitive to cold unfolding, and therefore very unstable in the bulk solution.

The opposite scenario of a protein that is stable against cold denaturation was also experimentally studied. For this purpose, lactate dehydrogenase was used. LDH was first dialyzed using a suitable kit (Pur-A-Lyzer Mega Dialysis Kit, MWCO 3.5 kDa, Sigma Aldrich, Milano, Italy) for 24 h at 277 K against 10 mM sodium citrate buffer at pH 6.5. The buffer was changed 3 times (the first 2 times every 3 h, whereas the last dialysis step was carried out overnight). The protein concentration in the dialyzed solution was measured through UV spectroscopy at 280 nm (6850 UV/VIS Spectrophotometer; Jenway, Stone, Staffordshire, UK), and the protein finally diluted to 10 μ g/ml in sodium citrate buffer at pH 6.5. At this pH value, LDH is stable in the bulk solution (the cold denaturation temperature is around 245 K (Hatley and Franks 1989)). For both protein formulations, the presence of 0.01 % w/v Tween 80 was also considered. The formulations were prepared using water for injection (Fresenius Kabi, Verona, Italy) and filtered using 0.2 μ m filters.

2.2.2. Freeze-Thaw Cycles

2 ml of the myoglobin formulations were dispensed into 4R vials (Nuova Ompi glass division, Stevanato Group, Piombino Dese, Italy) and stoppered with silicon stoppers (West Pharmaceutical Services, Milano, Italy). Four different freeze-thaw modalities were investigated: 1) cooling at 0.1 K/min followed by thawing at 0.5 K/min, 2) cooling at 0.1 K/min followed by thawing in a water bath at ambient temperature,

3) quenching in liquid nitrogen followed by thawing at 0.5 K/min, 4) quenching in liquid nitrogen followed by thawing in a water bath at ambient temperature. These 4 cycles were chosen because they explore the different combinations of slow (0.1 K/min) or fast (quenching) freezing, and slow (0.5 K/min) or fast (water bath) thawing. A LyoBeta 25 freeze-dryer (Telstar, Terrassa, Spain) was used to accurately control the freezing/thawing rates to 0.1 or 0.5 K/min.

A similar approach was used for LDH. Also in this case, four freeze-thaw modalities were investigated, again combining fast and slow procedures: 1) cooling at 0.5 K/min followed by thawing at 0.5 K/min, 2) cooling at 0.5 K/min followed by thawing in a water bath at ambient temperature, 3) quenching in liquid nitrogen followed by thawing at 0.5 K/min, 4) quenching in liquid nitrogen followed by thawing in a water bath at ambient temperature. In this case, for the cycles involving a rate-controlled ramp, a Revo freeze dryer (Millrock Technology, Kingston, NY) was used.

2.2.3. Analyses of Protein Stability

Protein stability after the freeze-thaw cycles was assessed by UV/VIS spectroscopy.

In the case of myoglobin, the protein formulation was first centrifuged at 13,000 rpm for 5 min (Heraeus Megafuge 8 Centrifuge Series, Thermo Fisher Scientific, Milano, Italy), and then analyzed at 410 nm (Multiskan Go Microplate Spectrophotometer, Thermo Fisher Scientific, Milano, Italy). For this analysis, Corning 96 well clear polystyrene microplates, with flat bottom and no surface treatment, were used (Sigma Aldrich, Milano, Italy). A decrease in absorbance at this wavelength, also known as the Soret band, is indicative of changes in the conformation of the heme group.

For LDH, the enzymatic activity after freeze-thawing was calculated from its ability to reduce NAD to NADH, as measured from the increase in absorbance at 450 nm. For this purpose, an activity assay kit was used (LDH activity assay kit, Sigma Aldrich, Milano, Italy). A standard curve built with 1.25 mM NADH standard was employed to calculate the amount of NADH generated in each well. Also in this case, the absorbance readings were carried out in a Multiskan Go microplate spectrophotometer, using Corning 96 well clear polystyrene microplates.

In all cases, the resulting values were averaged, and the standard deviations obtained were used to test for the significance of differences in the means. For this purpose, three-way ANOVA was performed (the three considered factors were freezing rate, thawing rate and presence of surfactants), and the outputs of this statistical analysis were further assessed by Tukey's HSD (honestly significant difference) test.

For both Mb and LDH, data will be normalized to the formulation before freeze/thaw, and reported as percentage of protein recovery.

3. Results and Discussion

3.1. Outputs of the Thawing Model for Protein Formulations

The model described in section 2.1 will be used in the following to provide insight into the role of the thawing process on protein stability.

In particular, the modeling of the thawing phase is started from the output of corresponding simulations of the freezing step. For this purpose, the model described in (Arsiccio et al. 2020a) is used, resulting in a design space like those shown in Figure 3. In these contour plots, the effect of cooling rate and nucleation temperature T_n on protein stability is shown. An 8 x 8 matrix of cooling rate x nucleation temperature

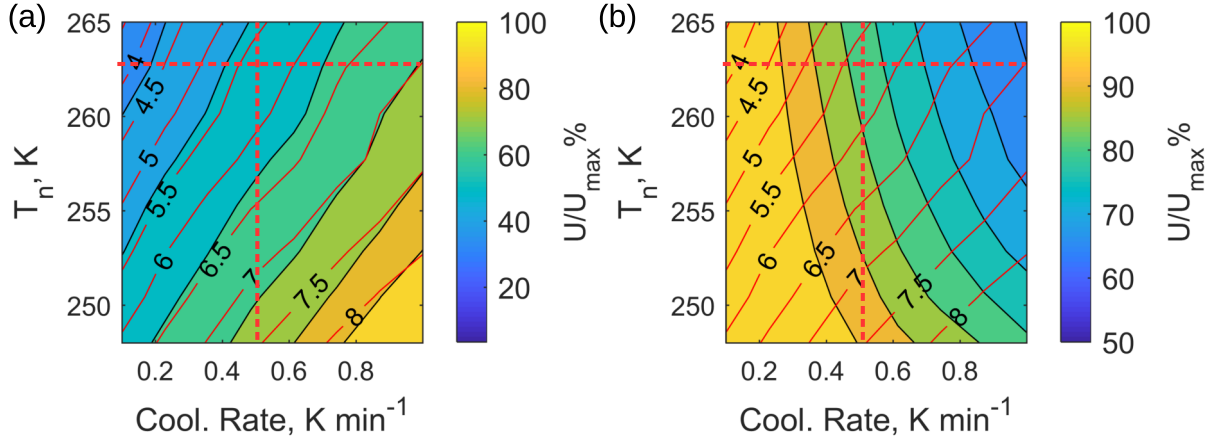


Figure 3. Design space for the freezing process, showing the effect of cooling rate and nucleation temperature on the percentage of unfolded protein molecules (U) relative to the maximum value in the design space (U_{max}). The red solid isocurves identify the conditions resulting in the same final extension of the ice-water surface area, shown in $\text{dm}^2 \text{g}^{-1}$ on the curves (the solvent mass is used as reference). The protein stability parameters of simulations 3 (panel a) and 4 (panel b) in Table 1 have been considered.

values in the range $[0.1 - 1 \text{ K min}^{-1}] \times [248 - 265 \text{ K}]$ has been built to obtain the design space, and the degree of protein unfolding computed for the selected combination of operating conditions. In particular, different colors correspond to different percentages of unfolded protein molecules, relative to the maximum value in the design space (U/U_{max}). The isocurves in red correspond to those conditions resulting in the same extension of the ice-water surface area.

Figure 3 shows the design space of freezing for conditions 3 and 4 in Table 1. As observed in our previous work (Arsiccio et al. 2020a), protein denaturation mostly occurs as a result of protein adsorption at the ice-water surface when the protein is stable in bulk, as for simulation 3. In this case, slow cooling rates or high nucleation temperature results in the best preservation of protein conformational stability, because these conditions minimize the extension of the ice-water surface area (see Figure 3a).

The opposite is true when the protein is unstable in bulk (simulation 4 in Table 1). In this case, the freezing process should be as fast as possible, to reduce the time spent by the protein in a liquid matrix at low viscosity, and high cooling rates are, therefore, beneficial (see Figure 3b).

The percentage of native (N) and unfolded (U) protein molecules at the end of freezing, and the final extension of the ice-water surface area, are used as inputs of the thawing model described in section 2.1. A representative output of a simulation of thawing is shown in Figure 4. The model first calculates the evolution of product temperature during thawing, as shown in Figure 4a. The formulation, initially frozen, is heated up, and its temperature increases steadily until a value close to 273 K. At this point, the heat removed by the melting of ice almost compensates for that supplied by the external environment, resulting in a plateau. When all the ice crystals have been removed, a change in slope is observed, and the temperature increases again till equilibrium with the external medium at 298 K. The evolution of the ice fraction X_{ice} as a function of temperature is shown in Figure 4b. The melting process starts already at 233 K but becomes very fast only around 273 K, resulting in the stiff change in excipient mass fraction in the amorphous phase x_s shown in Figure 4c. By contrast,

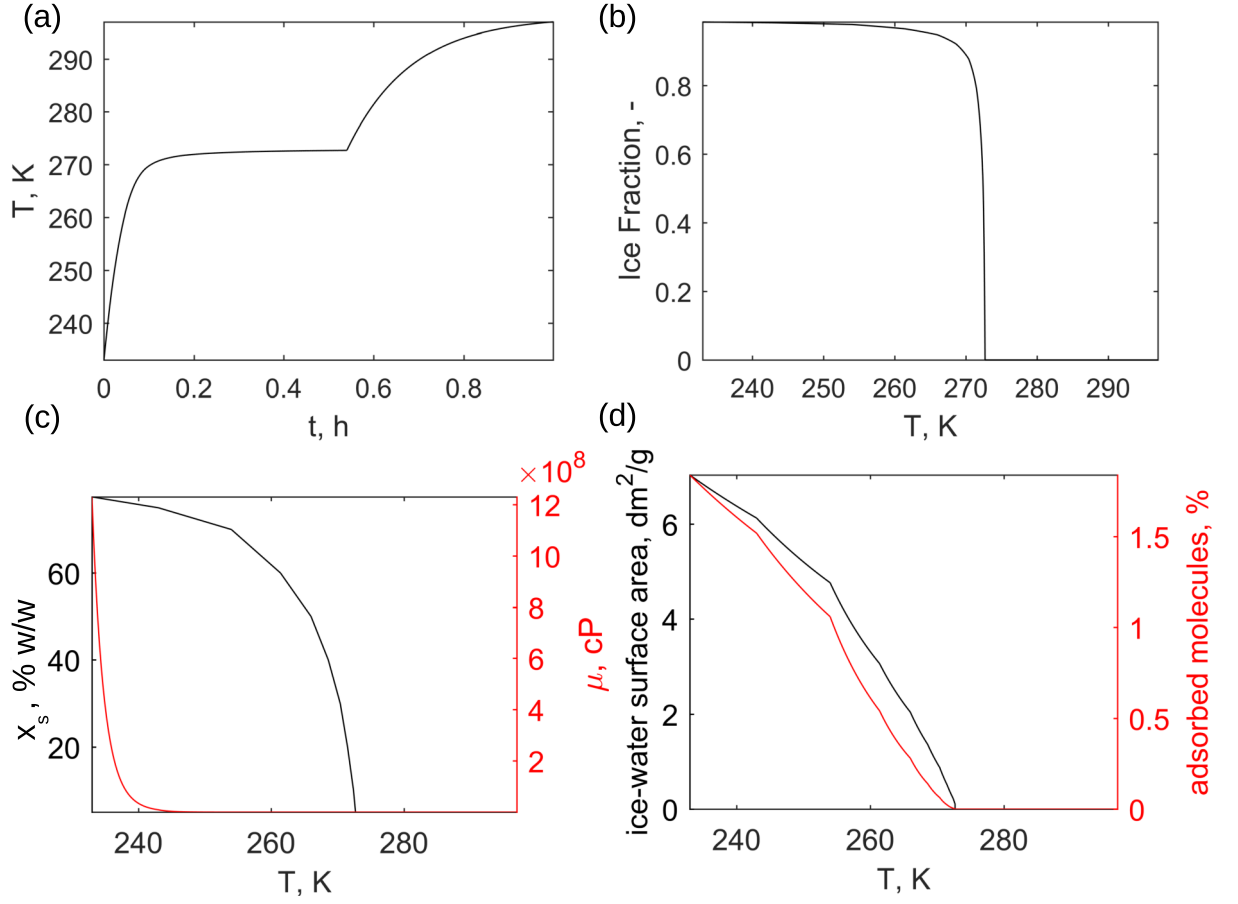


Figure 4. Representative output of a simulation of the thawing process. (a) Evolution of product temperature, (b) ice fraction as a function of time, (c) sucrose mass fraction x_s and viscosity of the freeze-concentrated phase μ , (d) ice-water surface area (expressed in $\text{dm}^2 \text{g}^{-1}$, using the solvent mass as reference) and percentage of adsorbed protein molecules. $K_v = 15 \text{ W m}^{-2} \text{K}^{-1}$ has been considered, while the initial extension of the ice-water surface area was calculated assuming a freezing process with $T_n = 263 \text{ K}$ and cooling rate equal to 0.5 K min^{-1} .

the viscosity (red curve in Figure 4c) starts to decline earlier, showing a marked change already around 241 K, which is the glass transition temperature of sucrose.

Finally, the extension of the ice-water surface area and the percentage of adsorbed protein molecules decrease during the melting process, as shown in Figure 4d.

When the evolution of all these variables during the thawing phase is known, it is also possible to compute the percentage of native and unfolded protein molecules as a function of time, as described in section 2.1. The degree of protein unfolding changes considerably if we consider different conditions of protein stability, i.e., if we move from simulation 1 to simulation 4 in Table 1. This is evident in Figure 5.

In the case of simulation 1 (Figure 5a), the protein is stable in bulk, and only minimally affected by external stresses. During thawing, a portion of the protein molecules that are desorbed from the ice-water surface refolds back to the native state, and there is an overall gain of protein conformational stability. The situation is reversed in the case of simulation 2 (Figure 5b). Here, the previously observed recovery of protein stability in the first part of the thawing process ($< 0.1 \text{ h}$), due to the decreased number of protein molecules adsorbed at the ice interface, is again present. However, the

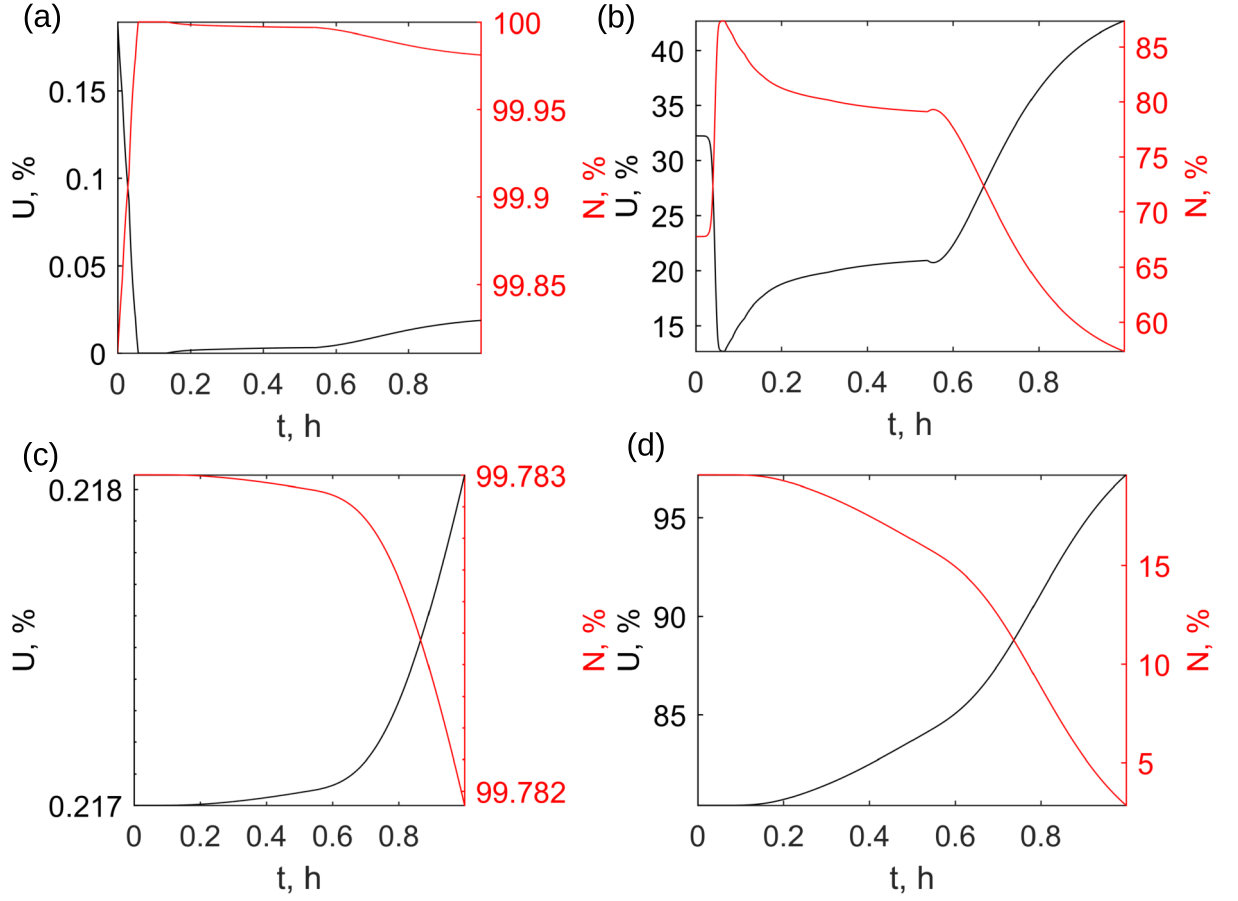


Figure 5. Representative evolution of the percentage of unfolded (U) and native (N) protein molecules during thawing, for the case of conditions 1 (a), 2 (b), 3 (c) or 4 (d) in Table 1. $K_v = 15 \text{ W m}^{-2} \text{ K}^{-1}$ has been considered, while the initial conditions, i.e. extension of the ice-water surface area and percentage of unfolded protein molecules, were calculated assuming a freezing process with $T_n = 263 \text{ K}$ and cooling rate equal to 0.5 K min^{-1} .

protein molecules are now unstable in bulk and undergo a quick denaturation process after the glass transition event (> 0.1 h) that becomes faster as the solution viscosity decreases. In this case, the thawing step is hugely detrimental to protein stability.

When the unfolding process is irreversible (as in the case of simulations 3 and 4), the protein recovery resulting from ice removal is absent (Figures 5c,d). In this case, the protein molecules that denatured during freezing because of adsorption onto the ice surface cannot convert back to the native fold. The percentage of unfolded protein molecules can only increase because of cold denaturation, but this process can be either negligible (Figure 5c) when the protein is stable in bulk, or extremely disruptive (Figure 5d) when a molecule prone to cold unfolding is considered.

3.2. A Design Space Approach for Selecting the best Thawing Conditions

Opposite cases of protein stability have been considered so far (sim. 1 to 4 in Table 1). A design space approach is here used to find the conditions that best preserve protein stability during a whole freeze-thaw cycle. The process variables that are selected as critical parameters are the cooling rate and nucleation temperature T_n during freezing, and the heat transfer coefficient K_v during thawing. These variables will be varied in the range $[0.1 - 1 \text{ K min}^{-1}]$, $[248 - 265 \text{ K}]$, or $[5 - 100 \text{ W m}^{-2} \text{ K}^{-1}]$, respectively. Cooling rate and nucleation temperature result in a different extension of the ice-water surface area, and a different velocity of the freezing process. By contrast, K_v affects the duration of the thawing phase (from up to 3 h when $K_v = 5 \text{ W m}^{-2} \text{ K}^{-1}$ to less than 10 minutes when $K_v = 100 \text{ W m}^{-2} \text{ K}^{-1}$).

A complete freeze-thaw cycle will be simulated. In particular, each simulation starts from a liquid solution at ambient temperature and no cryoconcentration effects, models its freezing to a solid matrix, and its melting back to the liquid state. In the case of simulations 1 and 2 in Table 1, the protein unfolding is completely reversible. In these conditions, the degree of protein denaturation is affected only by the starting and ending points of the process being investigated. By contrast, changes in path variables, such as cooling rate, nucleation temperature, and thawing rate, do not affect the final result. Since the initial and final points of the thermodynamic cycle here investigated are the same, i.e., a liquid solution at ambient temperature, the design space for simulations 1 and 2 would be trivial. Indeed, it would predict the same effect on protein stability for all possible choices of operating conditions. Attention will, therefore, be focused on simulations 3 and 4 in Table 1.

Two types of graphs will be built. In the first one (Figures 6a,c), the cooling rate and heat transfer coefficient K_v are varied at a fixed nucleation temperature of 263 K. In the second (Figures 6b,d), nucleation temperature and K_v are considered as variables, at a fixed cooling rate of 0.5 K min^{-1} . In practice, setting the nucleation temperature at 263 K, or the cooling rate at 0.5 K min^{-1} corresponds to move along the horizontal (fixed T_n) or vertical (fixed cooling rate) dashed lines represented in red on the contour plots shown in Figure 3. In all cases, an 8×8 matrix of possible combinations of operating conditions (cool. rate $\times K_v$ or $T_n \times K_v$) is built, and the extent of protein denaturation is computed for each point of the matrix. The meaning of the contour plots that are eventually obtained (Figure 6) is the same previously explained for Figure 3.

As it is possible to observe in Figures 6a,b, increasing the thawing rate slightly improves protein recovery when the protein is stable in the bulk solution (simulation 3), but this effect is minimal. This is in line with what had been previously observed in the

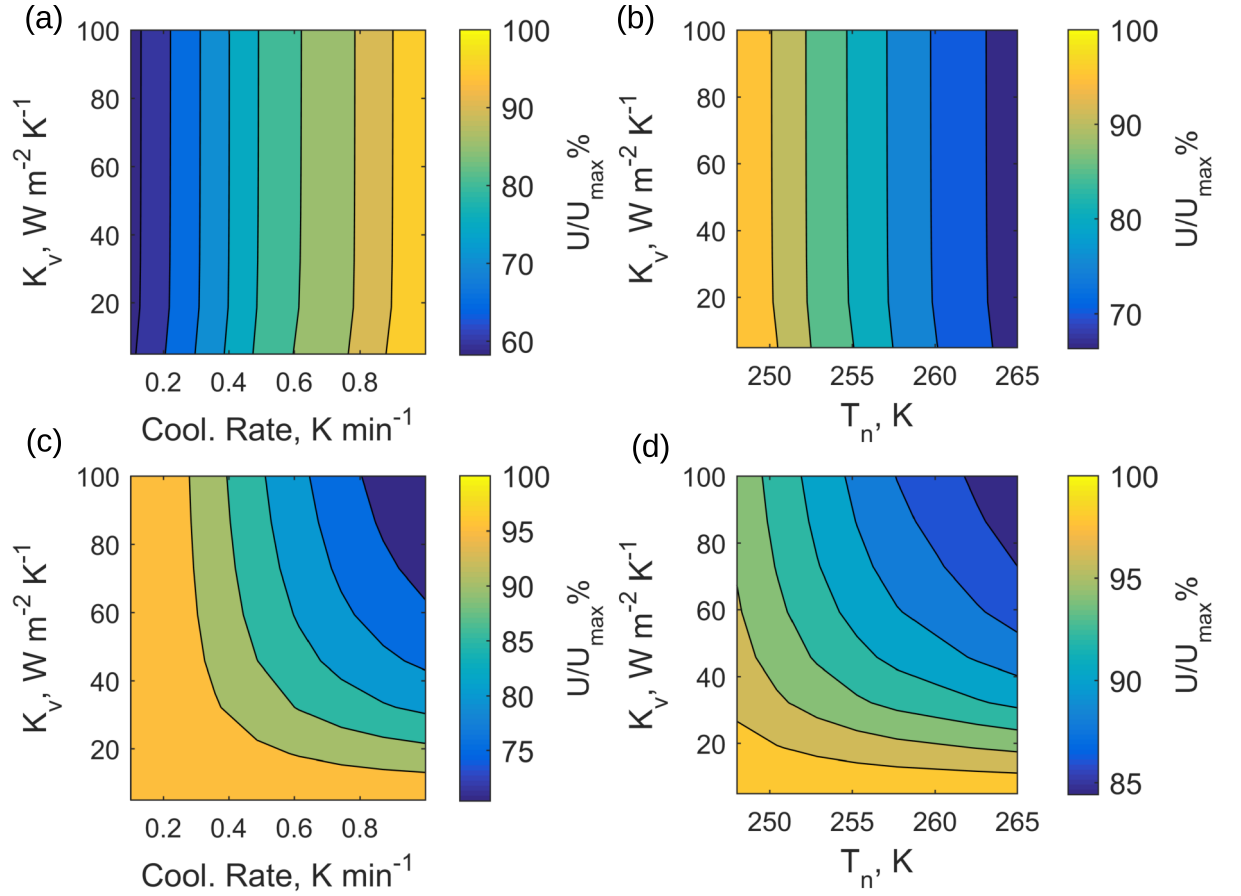


Figure 6. Design space for a freeze-thawing cycle, showing the effect of the cooling rate (panels a, c) or nucleation temperature (panels b, d) used during freezing, and of the heat transfer coefficient during thawing K_v on protein stability. In particular, the percentage of unfolded protein molecules (U) relative to the maximum value in the design space (U_{max}) has been selected as output variable for these contour plots. The protein stability parameters of simulations 3 (panels a, b), or 4 (panels c, d) in Table 1 have been considered.

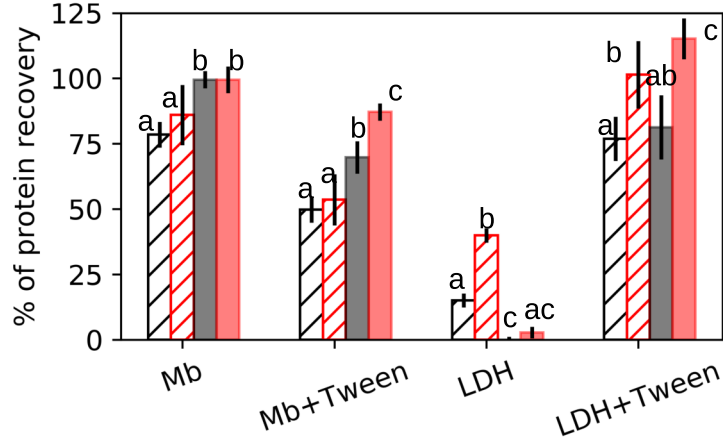


Figure 7. Recovery of Mb and LDH activity after freeze-thawing in citrate buffer only, or citrate buffer and 0.01 % w/v Tween 80. Different freeze-thawing modalities have been considered: slow freezing/slow thawing (black striped bars), slow freezing/fast thawing (red striped bars), fast freezing/slow thawing (black plain bars), fast freezing/fast thawing (red plain bars). The data here shown represent the average \pm standard deviation of at least 6 experiments. For a given formulation, bars that do not share a common letter (a, b or c) are statistically different according to the Tukey's HSD test ($p < 0.05$).

case of Figure 5c, where the extent of protein unfolding upon thawing was negligible. For a protein that is stable in the bulk solution, surface-induced denaturation prevails. Therefore, the degree of protein recovery is highest when the extension of the ice-water interface is smallest, i.e., at a low cooling rate and high nucleation temperature.

By contrast, the thawing rate should be maximized for optimal protein recovery when a molecule sensitive to cold denaturation is considered (simulation 4, Figures 6c,d). In this case, the higher the value of K_v is, the higher the percentage of native protein at the end of the cycle is, suggesting that the time spent in the liquid state is the crucial parameter for protein stability. If thawing is fast, the protein remains for a shorter time in a liquid matrix at a low viscosity. For the same reason, a high cooling rate (Figure 6c) and nucleation temperature (Figure 6d) are beneficial, as these conditions result in a fast formation of a cryo-concentrated matrix during freezing.

In summary, the following conclusions could be drawn: 1) For proteins that are stable in bulk, surface-induced denaturation prevails. The cooling rate used during freezing should be low, to promote the formation of large ice crystals. If possible, a controlled nucleation technique should be used to induce the formation of ice nuclei at high temperatures. A high thawing rate would be slightly beneficial, even though not crucial. 2) For cold-denaturation-prone molecules, the freezing and thawing processes should be as fast as possible. A high cooling and thawing rate would maximize protein recovery. The time spent by the formulation in the liquid state should be minimized.

The two opposite scenarios here investigated are extreme situations, which represent the upper and lower limit of any real system, and therefore allow a better understanding of protein behavior during freeze-thawing. In the following section, these theoretical considerations will be applied to the case of Mb at pH 3.7 and LDH at pH 6.5 as model proteins.

3.3. Comparison with Experimental Data

The two model proteins selected for this investigation show different stability against cold denaturation. Mb at pH 3.7 is extremely unstable in bulk, and we previously showed its tendency to unfold quickly when exposed to low temperatures (Arsiccio et al. 2020a). By contrast, LDH at neutral pH is stable up to low temperature in bulk, but extremely sensitive to ice-induced denaturation.

In line with the model results, we observed that fast freezing (black and red plain bars in Figure 7, corresponding to quench freezing in liquid nitrogen) was beneficial for Mb. In this case, the time spent by the protein in a liquid state at low viscosity should be minimized. Focusing on the Mb formulation without Tween 80, the ANOVA analysis suggests that the freezing rate is crucial. There is no statistical difference between the two tests at slow freezing rate (black and red striped bars in Figure 7, p -value > 0.05) and the two at fast freezing rate (black and red plain bars in Figure 7, p -value > 0.05). However, the statistical difference becomes significant when tests performed at different freezing rate are considered. For instance, the p -value drops to 3.2×10^{-5} when the combination slow freezing/slow thawing (black striped bar) is compared to fast freezing/slow thawing (black plain bar), indicating a significant difference in the means obtained.

While a fast freezing improved Mb recovery, the opposite was true for LDH, where a slow (0.5 K/min, black and red striped bars in Figure 7) freezing rate was beneficial when the protein was formulated in citrate buffer only. In this case, the best protein recovery was obtained when combining a slow freezing with a fast thawing (red striped bar in Figure 7), as also confirmed by the ANOVA analysis.

The presence of surfactants was also considered. The three-way ANOVA confirmed that the addition of a surfactant results in a statistically significant change in the results obtained. In particular, in the case of Mb, we observed (Arsiccio et al. 2020a) that Tween 80 was detrimental for protein stability. In line with these considerations, the protein recovery was always lower upon the addition of the surfactant to the Mb formulations. Only when the freeze-thaw cycle was extremely fast (cooling in liquid nitrogen, followed by thawing in water, red plain bar in Figure 7), the formulation with Tween behaved comparably to Mb in citrate buffer only. It is, therefore, possible to conclude that for a protein that is extremely unstable in the bulk solution, like Mb in the presence of Tween 80, both the freezing and thawing processes should be fast, in line with the contour plots shown in Figures 6c,d.

The effect of surfactants is considerably different for LDH as a model system. In this case, the addition of Tween 80 to the citrate buffer formulation largely improved protein recovery, as it counteracted ice-induced denaturation. This is evident because slow freezing at 0.5 K/min and quench cooling in liquid nitrogen affected protein stability to a similar extent upon the addition of Tween, as also confirmed by the Tukey’s HSD test (striped and plain black bars in Figure 7, for which $p > 0.05$ was obtained). In these conditions, only the thawing rate is important, and again a fast thawing rate is observed to be beneficial for protein stability (the red bars in Figure 7 for the LDH+Tween formulation show the highest values of protein recovery).

The experimental results here shown allow us to draw the same conclusions we previously inferred from the model outputs. In order to maximize protein recovery, the freezing rate should be fast for cold-denaturation-prone molecules, and slow for proteins that mostly denature at the ice surface. By contrast, a fast thawing rate is always beneficial.

4. Conclusions

In this work, a mathematical model has been proposed to describe the behavior of proteins during freeze-thawing. Both cold denaturation and surface-induced unfolding were taken into account, and the design space tool was used to obtain information about critical process parameters on protein stability. Model outputs allowed to infer that a low cooling rate during freezing is beneficial for proteins that are prone to unfold at the ice surface. In contrast, a high freezing rate improves the recovery of molecules that are extremely unstable in bulk. For all types of proteins, a high nucleation temperature, and a fast thawing rate should be beneficial according to the simulation results.

These same results were confirmed by an experimental investigation carried out on two model proteins, lactate dehydrogenase at pH 6.5 and myoglobin at pH 3.7, that have different tendencies to cold denature at low temperature. This suggests that the modeling approach, although simplified, can anyway reproduce the most important features of protein behavior during freeze-thawing.

It is the authors' opinion that a modeling approach, like the one here suggested, would substantially help in the selection of optimal operating conditions that maximize protein recovery after freeze-thaw. This would be particularly relevant for all those protein-based formulations that are stored in the frozen or freeze-dried state. Both robustness and process control may be improved, in line with the directives of QbD. This work represents a first step in this direction, and further work should be done to advance our knowledge in this field.

References

- Arsiccio A, Barresi AA, Pisano R. 2017. Prediction of ice crystal size distribution after freezing of pharmaceutical solutions. *Cryst Growth Des.* 17:4573–4581.
- Arsiccio A, Giorsello P, Marengo L, Pisano R. 2020a. Considerations on protein stability during freezing and its impact on the freeze-drying cycle: A design space approach. *J Pharm Sci.* 109:464 – 475.
- Arsiccio A, McCarty J, Pisano R, Shea JE. 2018. Effect of surfactants on surface-induced denaturation of proteins: Evidence of an orientation-dependent mechanism. *J Phys Chem B.* 122:11390–11399.
- Arsiccio A, McCarty J, Pisano R, Shea JE. 2020b. Heightened cold-denaturation of proteins at the ice-water interface. *J Am Chem Soc.* 142:5722–5730.
- Authelin JR, Rodrigues MA, Tchessalov S, Singh S, McCoy T, Wang S, Shalaeve E. 2020. Freezing of biologicals revisited: scale, stability, excipients, and degradation stresses. *J Pharm Sci.* 109:44–61.
- Bald WB. 1986. On crystal size and cooling rate. *J Microsc.* 143:89–102.
- Bhatnagar B, Zakharov BA, Fisyuk AS, Wen X, Karim FZ, Lee K, Seryotkin YV, Mogodi M, Fitch A, Boldyreva E, et al. 2019. Protein/ice interaction: High-resolution synchrotron X-ray diffraction differentiates pharmaceutical proteins from lysozyme. *J Phys Chem B.* 123:5690–5699.
- Bhatnagar BS, Pikal MJ, Robin HB. 2008. Study of the individual contributions of ice formation and freeze-concentration on isothermal stability of lactate dehydrogenase during freezing. *J Pharm Sci.* 97:798–814.
- Cao E, Chen Y, Cui Z, Foster PR. 2003. Effect of freezing and thawing rates on denaturation of proteins in aqueous solutions. *Biotechnol Bioeng.* 82:684–690.
- Chang BS, Kendrick BS, Carpenter JF. 1996. Surface-induced denaturation of proteins during freezing and its inhibition by surfactants. *J Pharm Sci.* 85:1325–1330.

- Chang BS, Randall CS. 1992. Use of subambient thermal analysis to optimize protein lyophilization. *Cryobiology*. 29:632–656.
- Davidovic M, Mattea C, Qvist J, Halle B. 2009. Protein cold denaturation as seen from the solvent. *J Am Chem Soc*. 131:1025–1036.
- Eckhardt BM, Oeswein JQ, Bewley TA. 1991. Effect of freezing on aggregation of human growth hormone. *Pharm Res*. 8:1360–1364.
- Fang R, Tanaka K, Mudhivarthi V, Bogner RH, Pikal MJ. 2018. Effect of controlled ice nucleation on stability of lactate dehydrogenase during freeze-drying. *J Pharm Sci*. 107:824–830.
- Hatley RHM, Franks F. 1989. The cold-induced denaturation of lactate dehydrogenase at sub-zero temperatures in the absence of perturbants. *FEBS Lett*. 257:171–173.
- Heller MC, Carpenter JF, Randolph TW. 1996. Effects of phase separating systems on lyophilized hemoglobin. *J Pharm Sci*. 85:1358–1362.
- Heller MC, Carpenter JF, Randolph TW. 1997. Manipulation of lyophilization induced phase separation: Implications for pharmaceutical proteins. *Biotechnol Prog*. 13:590–596.
- Honig P. 2013. Principles of sugar technology. Elsevier Science.
- Jiang S, Nail SL. 1998. Effect of process conditions on recovery of protein activity after freezing and freeze-drying. *Eur J Pharm Biopharm*. 45:249 – 257.
- Kasper JC, Friess WF. 2011. The freezing step in lyophilization: Physico-chemical fundamentals, freezing methods and consequences on process performance and quality attributes of biopharmaceuticals. *Eur J Pharm Biopharm*. 78:248–263.
- Lee HJ, McAuley A, Schilke KF, McGuire J. 2011. Molecular origins of surfactant-mediated stabilization of protein drugs. *Adv Drug Deliv Rev*. 63:1160–1171.
- Longinotti MP, Corti HR. 2008. Viscosity of concentrated sucrose and trehalose aqueous solutions including the supercooled regime. *J Phys Chem Ref Data*. 37:1503–1515.
- Lopez CF, Darst RK, Rossky PJ. 2008. Mechanistic elements of protein cold denaturation. *J Phys Chem B*. 112:5961–5967.
- Matysiak S, Debenedetti PG, Rossky PJ. 2012. Role of hydrophobic hydration in protein stability: A 3D water-explicit protein model exhibiting cold and heat denaturation. *J Phys Chem B*. 116:8095–8104.
- Pikal-Cleland KA, Rodriguez-Hornedo N, Amidon GL, Carpenter JF. 2000. Protein denaturation during freezing and thawing in phosphate buffer systems: Monomeric and tetrameric β -galactosidase. *Arch Biochem Biophys*. 384:398–406.
- Pincock RE, Kiovsky TE. 1966. Kinetics of reactions in frozen solutions. *J Chem Educ*. 43:358.
- Pisano R. 2019. Alternative methods of controlling nucleation in freeze drying. In: Ward KR, Matejtschuk P, editors. *Lyophilization of Pharmaceuticals and Biologicals: New Technologies and Approaches*. New York, NY: Springer New York; p. 79–111.
- Privalov PL. 1990. Cold denaturation of proteins. *Crit Rev Biochem Mol Biol*. 25:281–305.
- Privalov PL. 1997. Thermodynamics of protein folding. *J Chem Thermodyn*. 29:447–474.
- Sarciaux JM, Mansour S, Hageman MJ, Nail SL. 1999. Effects of buffer composition and processing conditions on aggregation of bovine IgG during freeze-drying. *J Pharm Sci*. 88:1354–1361.
- Schwegman JJ, Carpenter JF, Nail SL. 2009. Evidence of partial unfolding of proteins at the ice/freeze-concentrate interface by infrared microscopy. *J Pharm Sci*. 98(9):3239 – 3246.
- Searles JA, Carpenter JF, Randolph TW. 2001. The ice nucleation temperature determines the primary drying rate of lyophilization for samples frozen on a temperature-controlled shelf. *J Pharm Sci*. 90:860 – 871.
- Strambini GB, Gabellieri E. 1996. Proteins in frozen solutions: Evidence of ice-induced partial unfolding. *Biophys J*. 70:971–976.
- Young FE, Jones FT. 1949. Sucrose hydrates. The sucrose-water phase diagram. *J Phys Chem*. 53:1334–1350.
- Yu LX. 2008. Pharmaceutical quality by design: Product and process development, understanding, and control. *Pharm Res*. 25:781–791.
- Yu LX, Amidon G, Khan MA, Hoag SW, Polli J, Raju GK, Woodcock J. 2014. Understanding pharmaceutical quality by design. *AAPS J*. 16:771–783.

Zwanzig R. 1997. Two-state models of protein folding kinetics. *Proc Natl Acad Sci.* 94:148–150.